The Cav1.2 N terminus contains a CaM kinase site that modulates channel trafficking and function

ARTICLE *in* PFLÜGERS ARCHIV - EUROPEAN JOURNAL OF PHYSIOLOGY · MAY 2014

Impact Factor: 4.1 · DOI: 10.1007/s00424-014-1538-7 · Source: PubMed

4 AUTHORS, INCLUDING:

Brett Simms
The University of Calgary
14 PUBLICATIONS **379** CITATIONS
SEE PROFILE

Renata Rehak
The University of Calgary
17 PUBLICATIONS **722** CITATIONS
SEE PROFILE

Pflugers Arch - Eur J Physiol
DOI 10.1007/s00424-014-1538-7

The Cav1.2 N terminus contains a CaM kinase site that modulates channel trafficking and function

Brett A. Simms · Ivana A. Souza · Renata Rehak · Gerald W. Zamponi

Received: 25 April 2014 / Revised: 12 May 2014 / Accepted: 14 May 2014

Abstract The L-type voltage-gated calcium channel Cav1.2 and the calcium-activated CaM kinase cascade both regulate excitation transcription coupling in the brain. CaM kinase is known to associate with the C terminus of Cav1.2 in a region called the PreIQ-IQ domain, which also binds multiple calmodulin molecules. Here we identify and characterize a second CaMKII binding site in the N terminus of Cav1.2 that is formed by a stretch of four amino residues (cysteine–isoleucine–serine–isoleucine) and which regulates channel expression and function. By using live cell imaging of tsA-201 cells we show that GFP fusion constructs of the CaMKII binding region, termed $N_{2B\text{-}II}$ co-localize with mCherry-CaMKII. Mutating CISI to AAAA ablates binding to and colocalization with CaMKII. $Cav1.2_{\text{-AAAA}}$ channels show reduced cell surface expression in tsA-201 cells, but interestingly, display an increase in channel function that offsets the trafficking deficit. Altogether our data reveal that the proximal N terminus of Cav1.2 contains a CaMKII binding region which contributes to channel surface expression and function.

Keywords L-type calcium channel · Calmodulin kinase · N terminus · Cav1.2 · Surface expression

Abbreviations

CaMK	Calmodulin kinase
CaMKK	Calmodulin kinase kinase
CaM	Calmodulin
CDF	Calcium-dependent facilitation
CDI	Calcium-dependent inactivation
VDF	Voltage-dependent facilitation

Introduction

Neuronal voltage-gated calcium channels are important for synaptic transmission, gene transcription and neuronal development [6], while their dysfunction can cause epilepsy, ataxia, migraine and pain [35]. The L-type calcium channel Cav1.2 is important in brain tissue for gene expression and activates the transcription factors CREB and NFAT [15, 16]. Cav1.2 is essential for emotional learning through its activity in the amygdala and anterior cingulate cortex [23, 26]. Not dissimilar from Cav1.2 channels, the calcium activated cascade comprising calmodulin kinase (CaMK) and calmodulin kinase kinase (CaMKK) participates in emotional learning [4, 30].

At the molecular level neuronal Cav1.2 channels and CaMKII regulate CREB activation following brief depolarizations in a manner which is intimately tied to open probability of the channel [40]. For the Cav2 family of voltage-gated calcium channels calmodulin (CaM) and CaM kinase modulate a process known as calcium-dependent facilitation (CDF), which functions to upregulate channel conductance in low intracellular calcium, but which is in competition with calcium-dependent inactivation (CDI) when levels of calcium rise [11, 27]. For L-type calcium channels two different types of CDI are evident [3, 8, 12] and although CaMK is involved in facilitating these channels, CDF is only possible when the

B.A. Simms and I.A. Souza contributed equally to this study.

Electronic supplementary material The online version of this article (doi:10.1007/s00424-014-1538-7) contains supplementary material, which is available to authorized users.

B. A. Simms · I. A. Souza · R. Rehak · G. W. Zamponi (✉)
Department of Physiology and Pharmacology, Hotchkiss Brain Institute, University of Calgary, 3330 Hospital Drive NW, Calgary, AB T2N 4N1, Canada
e-mail: Zamponi@ucalgary.ca

Published online: 28 May 2014

C-terminal IQ region of the channel is mutated [46]. Nevertheless, in the presence of the IQ mutation, removal of CaMKII binding from the neighboring PreIQ-IQ region quells frequency-dependent facilitation of Cav1.2 channels in calcium, thus suggesting that under certain conditions CaMKII may modulate Cav1.2 CDF [22]. It is from the work of Hudmon and colleagues [22] that the presence of an N-terminal CaMKII site in Cav1.2 was first demonstrated through the use of GST pulldowns, although no function was ever described. While exploring CDI of Cav1.2 channels in a recent study, we narrowed the site of CaMKII interaction to the proximal N terminus of the channel. Here using a combination of biochemistry, immunocytochemistry and electrophysiology we identify the precise location of this N-terminal CaMKII site and describe its effects on subcellular trafficking and function of the Cav1.2 channel.

Methods

cDNA constructs

Wild type (WT) rat calcium channel subunit cDNAs encoding Cav1.2 (α1C), Cavβ2a, Cavβ1b and Cavα2δ1 subunits, as well as the pMT2 vector were donated by Dr. Terry Snutch (University of British Columbia, Vancouver, BC). The mCherry-α-CaMKII was a gift from Dr. Paul De Koninck (Universite of Laval, Quebec, QC, Canada) and has been previously described [21]. The HA tagged version of Cav1.2 [1] has been previously described. Cav1.2 channels used in this work have aspartic acid at amino acid 57. The origins of the clones used or GenBank™ accession numbers where available are as follows: Cav1.2 [M67515], Cavβ1b [NM017346], Cavβ2a [31], Cavα2δ1 [AF286488], α-CaMKII [NM_012920.1]. HA and non-tagged Cav1.2$_{-AAAA}$ channels were created by cloning their respective synthesized sequences (Genscript) into ClaI/BsrGI. Cav1.2 N-terminal GFP fusion proteins, for which the construction of PreIQ-IQ, Nterm, N_1, N_2, N_{2A}, N_{2B}, and $N_{2B\text{-}II}$ has been previously described [34], were cloned into N1-GFP (Clontech) using *Bam*HI/*Xho*I. Annealing reactions (95° for 10 min, followed by cooling to 20° over a 25-min period) of complimentary primers (20 pmol/primer) followed by cloning were used to generate the following GFP fusion constructs (primers used):

$N_{2B\text{-}II\text{-}R}$: (TCGAGATGACTCTGAAGAACCCCATCAG GAGGGCACGCATCAGCATTGTTG AATGGAAAGGG/ GATCCCCTTTCCATTCAACAATGCTGATGCGTGCCC TCCTGATGGGGTTCTTCAGAGTCATC),

$N_{2B\text{-}II\text{-}RR}$: (TCGAGATGACTCTGAAGAACCCCATC AGGAGGGCACGCATCCGCATTGTTG AATGGAAAGG G/GATCCCCTTTCCATTCAACAATGCGGATGCGTGC CCTCCTGATGGGGTTCTTCAGAGTCATC),

$N_{2B\text{-}II\text{-}RARA}$: (TCGAGATGACTCTGAAGAACCCCATC AGGAGGGCACGCGCCCGCGCTGT TGAATGGAAA GGG/GATCCCCTTTCCATTCAACAGCGCGGGCGCGT GCCCTCCTGATGGGGTTCTTCAGAGTCATC),

$N_{2B\text{-}II\text{-}AAAA}$: TCGAGATGACTCTGAAGAACCCCATC AGGAGGGCAGCTGCCGCAGCTGT TGAATGGAAA GGG/GATCCCCTTTCCATTCAACAGCTGCGGCAGCT GCCCTCCTGATGGGGTTCTTCAGAGTCATC.

All cDNAs were sequenced after cloning to verify fidelity.

Tissue culture and transient transfection of tsA-201 cells

Human embryonic kidney tsA-201 cells were cultured and transiently transfected using the calcium phosphate method as described previously [18]. For Western blotting and electrophysiology experiments, 3 μg of each cDNA were transfected in 60-mm or 10-cm plates. For imaging experiments 500 ng of each HA tagged Cav1.2 channels, and Cavβ, as well as Cavα2δ1 subunits were transfected. For imaging experiments using GFP, or mCherry fusion proteins, 250 ng of each construct were transfected in 35-mm MatTEK plates. Cells were grown at 37 °C for 48–72 h after transfection to 75–85 % confluence, with the exception of cells for electrophysiology which were kept to low confluence.

Immunoprecipitation and Western blotting

Cultured tsA-201 cells were transiently transfected as described above with cDNAs for immunoprecipitation assays and were lysed with a modified RIPA buffer (in mM; 50 Tris, 130 NaCl, 0.2 % triton X-100, 0.2 % NP-40, 0.5 Ca^{2+}, pH 7.4). Detailed methods for cell preparation for immunoblots have been described previously [34]. For immunoprecipitation 1 μg of GFP (Abcam-1218) antibody was used. Western blot analysis was performed using one of the following: 1:500 anti-HA (Roche), 1:1,000 anti-GFP (Santa-Cruz-8334), 1/1000 anti-mCherry (Abcam-1C51), or 1:1,000 α-CaMKII (Santa Cruz-9035). Where necessary, membranes were stripped as previously described [34] and inputs taken from whole cell samples representing 2.5 % of total protein and probed for one of the following: Na/K ATPase (Abcam-7671), GFP (Santa Cruz-8334), mCherry (Abcam-1C51), α-CaMKII (Santa Cruz-9035), HA (Roche). GE Healthcare horseradish peroxidase-linked secondary antibodies of appropriate species (mouse, rabbit and rat) were used at 1:5,000 dilution.

Cell surface biotinylation

Cells transfected with HA tagged Cav1.2 channel subunits were washed and incubated with cold HBSS on ice for 20 min to stop trafficking of proteins. Surface proteins were biotinylated with 1 mg/ml EZ-Link Sulfo-NHS-SS-Biotin (Thermo

Scientific) for 1 h on ice. The biotinylation reaction was quenched with cold 100 mM glycine in HBSS for 15 min and cells were washed in HBSS and lysed in modified RIPA buffer for 30 min. The protein concentration of lysates was measured using the BioRad protein assay and 100 μl of Neutravidin beads (Thermo Scientific) were added to 3 mg lysates. After incubation for 1.5 h at 4 °C, beads were washed four times with the same lysis buffer and biotinylated proteins eluted with 2× Laemmli sample buffer. Biotinylated fraction and lysates were resolved by SDS-PAGE followed by Western blot analysis. Image J (National Institute of Health) was used to quantify the integrated density (amount of protein). For each blot the background signal was subtracted from experimental values to obtain real sample values. Biotinylated HA signal was then divided by biotinylated Na/K ATPase to control for gel loading. Mutant channel expression at the cell surface is expressed as a ratio of WT-Cav1.2.

Confocal imaging

Cultured tsA-201 cells, transfected with HA-tagged Cav1.2 channels, were fixed with 4 % paraformaldehyde in HBSS 72 h after transfection and immunostained with rat anti-HA antibody (1/500) and then Alexa Fluor 594-conjugated goat α-rat IgG antibody (Molecular Probes; 1/1,000). For live cell imaging of GFP and mCherry fusion proteins tsA-201 cells were grown for 48 h post-transfection, and then placed in HBSS. Images were acquired with a Zeiss LSM-510 Meta confocal microscope using a 63× 1.4NA oil immersion lens in the inverted position. Co-localization experiments using GFP and mCherry constructs were performed using dual excitation (488 and 543) and emission filters BP505-530 and LP650. Bleed-through was assessed with transfected cells expressing only one fluorescent protein. Detector gain, pinhole aperture, laser excitation and scanning speed were left unchanged for all samples unless otherwise indicated.

Voltage-clamp recordings

Glass cover slips carrying cells with WT or Cav1.2$_{-AAAA}$ channels (no HA tag) were transferred to a 3.5-cm culture dish (Corning) containing external recording solution consisting of a 20-mM barium chloride as described previously [34]. Where necessary, the L-type calcium channel agonist (±) BayK 8644 (Sigma-Aldrich) was added (1 μM). Microelectrode patch pipettes were pulled and polished using a DMZ-Universal Puller (Zeitz Instruments GmbH). A cesium methanesulfonate internal pipette solution was used as described previously [34]. Whole-cell patch clamp recordings were performed in voltage-clamp mode using an Axopatch 200B amplifier (Axon Instruments) linked to a personal computer with pCLAMP software version 9.2. Series resistance

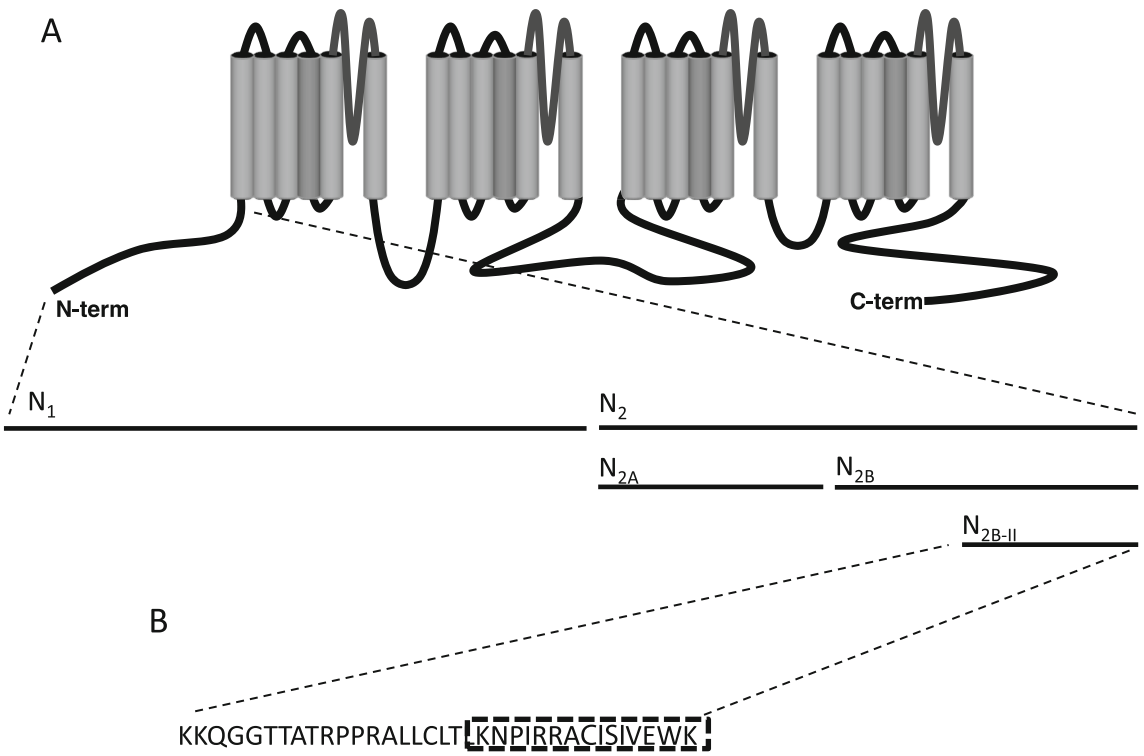

Fig. 1 Cav1.2 N-terminal GFP fusion proteins. **a** Cartoon of the four domain Cav1.2 structure highlighting N-terminal GFP fusion proteins used. **b** The primary amino acid sequence of the N_{2B-II} portion of the Cav1.2 N terminus. The *hatched box* denotes the approximate location of the α-CaMKII interaction site mapped by our previous work. *Bolded* residues highlight the α-CaMKII interaction site identified here

was compensated by 85 %, leak currents were negligible, and the data were filtered at 5 kHz.

Individual GFP expressing cells were held at −100 mV and pulsed in 10-mV increments from −60 to +60 mV for a period of 1 s to determine the current/voltage (IV) relationship. Individual pulses/runs were separated by 15 s to enable full channel recovery in all experiments unless indicated. All stable cells with detectable inward current at 0 mV were used to calculate current density. For voltage-dependent facilitation, cells were held at −80 mV and pulsed to 0 mV (50 ms) to determine non-facilitated current, returned to −80 mV (1 s) then stepped to +120 mV (200 ms), followed by a brief 10-ms step to −80 mV, and a final test pulse to 0 mV (50 ms) to determine facilitated current.

Data analysis

All electrophysiological data were analyzed using Clampfit version 10.2 (Axon Instruments) and fit in Origin 9 (Origin Lab Corporation). Statistical analyses for both biochemical and electrophysiological data were carried out using Origin 9. All sample means are reported±SEM. Statistically significant differences between means were assessed using Student's *t*-test, or one-way analysis of variance (ANOVA) at 95 % confidence level as appropriate.

Results

A proximal C–I–S–I sequence in the N terminus of Cav1.2 forms the α-CaMKII binding site

Several intracellular linkers including the N terminus of Cav1.2 have been shown to bind CaMKII with unknown functional consequence [22]. In previous work we narrowed the site of α-CaMKII binding to the proximal N terminus of Cav1.2, but did not explore this interaction further [34]. Because CaMK is important for CDF of

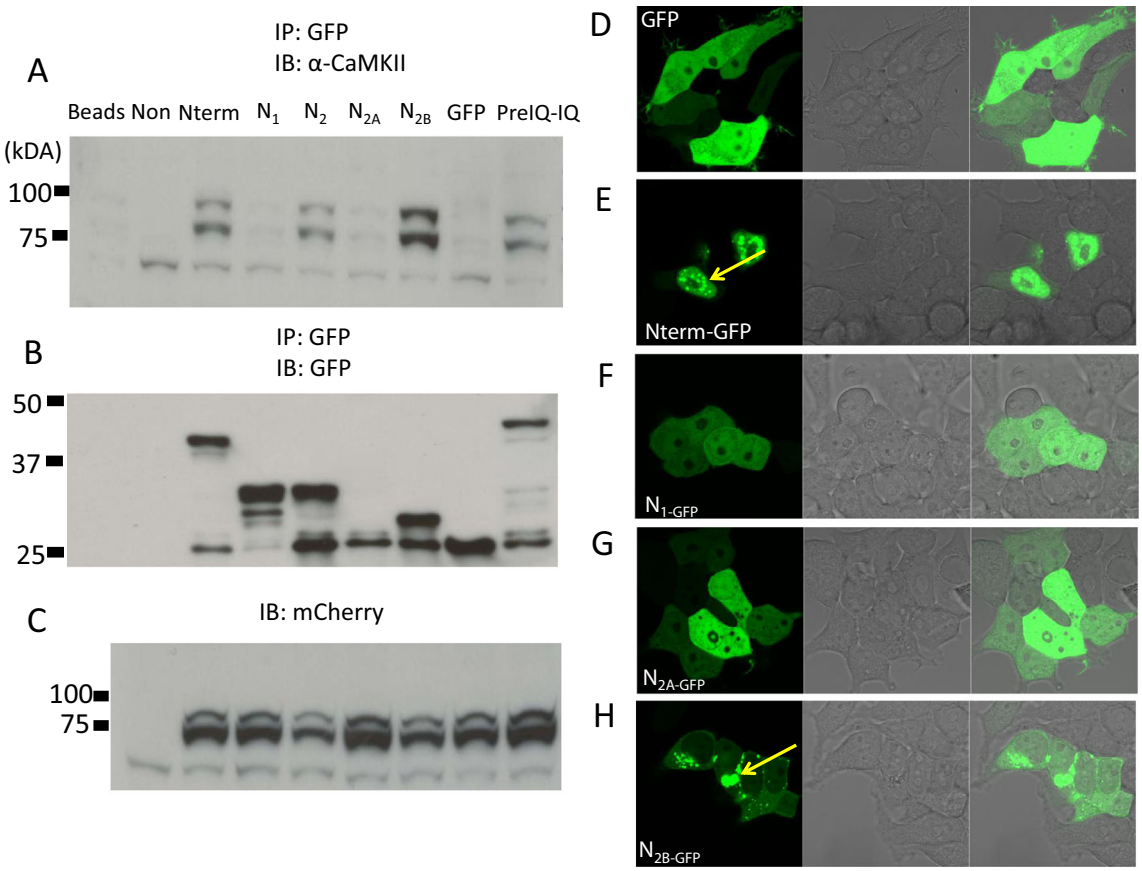

Fig. 2 α-CaMKII binding occurs within the N_{2B} region of the Cav1.2 N terminus and causes aggregate formation in tsA-201 cells. **a** Coimmunoprecipitation experiments of mCherry-α-CaMKII and N-terminal GFP fusion proteins (predicted sizes: Nterm, 41 kDa; N_1, 34 kDa; N_2, 33 kDa; N_{2A}, 30 kDa; and N_{2B}, 31 kDa) or PreIQ-IQ positive control (predicted size 43 kDa). Immunoprecipitates of GFP and controls (nontransfected/beads alone) were run on SDS-PAGE and blotted for α-CaMKII. **b** Membranes were then stripped and re-probed for GFP. **c** Western blot of α-CaMKII in lysate. **d** Confocal images of live tsA-201 cells expressing GFP, Nterm-GFP (**e**), N_1-GFP (**f**), N_{2A}-GFP (**g**) and N_{2B}-GFP (**h**). Images of GFP fusion proteins were acquired by exciting at 488 and emissions band-pass filtering at 505–530. Each experiment is representative of three successful attempts and yellow arrows highlight aggregates

Cav2 [11, 28], and CREB-dependent gene transcription of both Cav1 [2] and Cav2 channels [40, 41], we focused on further understanding the physiological role of this novel CaMKII site.

Using coimmunoprecipitation experiments and live cell imaging of GFP fusion proteins of the Cav1.2 N terminus (Fig. 1) we first verified the existence of the proximal N terminus α-CaMKII interaction site. Figure 2a–c shows that all N-terminal constructs containing the proximal N_{2B} portion (i.e., Nterm, N_2 and N_{2B}) of Cav1.2 coimmunoprecipitate mCherry-α-CaMKII, as does the positive control PreIQ-IQ-GFP. Live cell imaging in tsA-201 cells (Fig. 2d–h) shows that N_{2B} containing GFP fusion proteins (i.e., Nterm and N_{2B}) form aggregates, while all other N-terminal fusion proteins do not. Our previous work [34] has attributed this aggregation of N-terminal fusion proteins to an association with CaMK, thus providing a useful assay to examine CaMK interactions in live cells.

We next focused on pinpointing the exact residues by which α-CaMKII binds the proximal N terminus of Cav1.2. Figure 3 demonstrates that replacing four sequential residues cysteine–isoleucine–serine–isoleucine (CISI, 117–120 aa) with alanines, prevents binding of $N_{2B\text{-}II}$-GFP to mCherry-α-CaMKII. A single mutant C117R or double mutant C117R/S119R version of $N_{2B\text{-}II}$-GFP both retain binding to α-CaMKII, necessitating mutation of the adjacent isoleucines (Fig. S1). It is interesting to note that disruption of α-CaMKII binding to the PreIQ-IQ region of the C terminus of Cav1.2 also requires multiple mutations (TVGKFY-AAAAAA), suggesting that channel interactions with α-CaMKII are inherently resilient [22]. Nevertheless, given the loss of mCherry-α-CaMKII binding to $N_{2B\text{-}II\text{-}AAAA}$-GFP we expected that the latter fusion protein would no longer aggregate in live tsA-201 cells. Indeed, as shown in Fig. 4b, $N_{2B\text{-}II}$-GFP aggregates and co-localizes with mCherry-α-CaMKII in live cells whereas $N_{2B\text{-}II\text{-}AAAA}$-GFP does not (Fig. 4d). Altogether, our biochemical and immunocytochemical results illustrate that four residues in the proximal N terminus of Cav1.2 bind and promote co-localization with α-CaMKII.

Cav1.2 channels lacking an N-terminal α-CaMKII binding site have reduced surface expression but not reduced function

In order to determine the function of the α-CaMKII site in the N terminus of Cav1.2, we applied a combination of surface protein biotinylation, confocal imaging and electrophysiological analysis. Figure 5a shows that externally tagged WT-

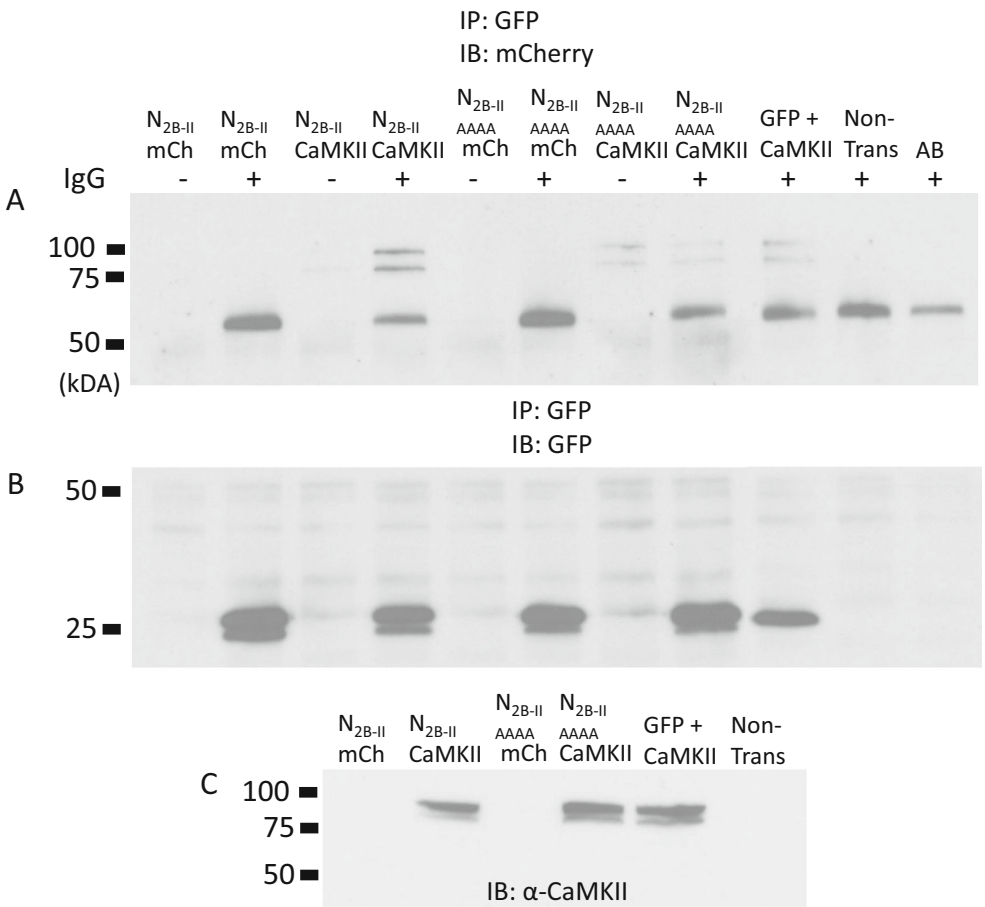

Fig. 3 Mutagenesis of $N_{2B\text{-}II}$ identifies four residues (CISI) important for binding α-CaMKII. **a** Coimmunoprecipitation experiments of mCherry (*mCh*), or mCherry-α-CaMKII with one of $N_{2B\text{-}II}$-GFP, or $N_{2B\text{-}II\text{-}AAAA}$-GFP (predicted sizes of both constructs are 29 kDa). Immunoprecipitates of GFP constructs and controls (nontransfected, or antibody [*AB*]) were run on SDS-PAGE and blotted for mCherry. **b** Membranes were then stripped and re-probed for GFP. **c** Western blot of α-CaMKII in lysate. This experiment is representative of two successful experiments

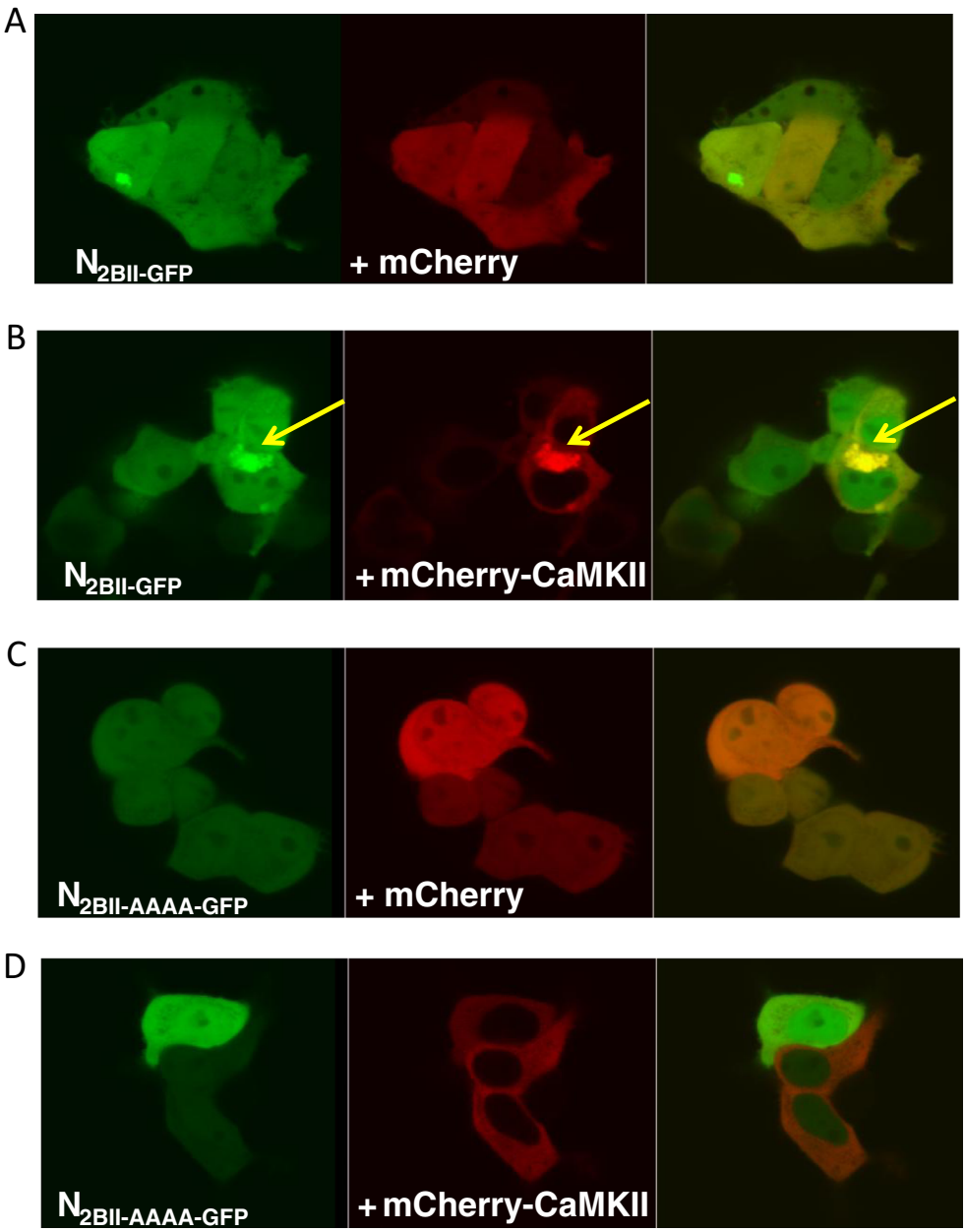

Fig. 4 mCherry-α-CaMKII requires CISI sequence for co-localization with $N_{2B\text{-}II}$ in tsA-201 cells. **a** Confocal images of live tsA-201 cells expressing mCherry and $N_{2B\text{-}II}$-GFP, mCherry-α-CaMKII and $N_{2B\text{-}II}$-GFP (**b**), mCherry and $N_{2B\text{-}II\text{-}AAAA}$-GFP (**c**), mCherry-α-CaMKII and $N_{2B\text{-}II\text{-}AAAA}$-GFP (**d**). Images of GFP and mCherry fusion proteins were acquired by dual excitation (488 and 543) and emissions filtered at 505–530 (BP) and 650 (LP). This experiment is representative of two successful experiments

Cav1.2 channels, in the presence of auxiliary subunits, express well both at the cell surface and intracellularly (Fig. S2a). Externally tagged HA-Cav1.2$_{\text{-AAAA}}$ channels, on the other hand, have much lower surface expression under the same conditions (non-permeabilized cells, Fig. 5b), but show robust total protein expression (permeabilized cells, Fig. S2b). Surface protein biotinylation studies support these observations and demonstrate that Cav1.2$_{\text{-AAAA}}$ expresses much less than WT-Cav1.2 channels in the surface pool (Fig. 5c). Normalized quantification of channel biotinylation illustrates that Cav1.2$_{\text{-AAAA}}$ expresses significantly less at the cell surface (0.46±0.17, *p=0.02 by Students *t*-test) compared to WT-Cav1.2 channels, whereas total protein expression levels were similar. These data indicate that α-CaMKII may regulate the subcellular trafficking of Cav1.2 channels.

We next used electrophysiology to test whether Cav1.2$_{\text{-AAAA}}$ whole cell current density was altered by the reduction in the surface pool of channels. Unexpectedly, Cav1.2$_{\text{-AAAA}}$ current density was not statistically different from WT-Cav1.2 channels in the presence of either Cavβ1b, or Cavβ2a auxiliary subunits (Fig. 5e). Because whole cell current amplitude is governed by three factors (numbers of channels at the cell surface, open probability and single channel conductance), this result implies that Cav1.2$_{\text{-AAAA}}$ channels exhibit augmented either an increase in maximum open probability or in conductance which would offset their poor surface expression.

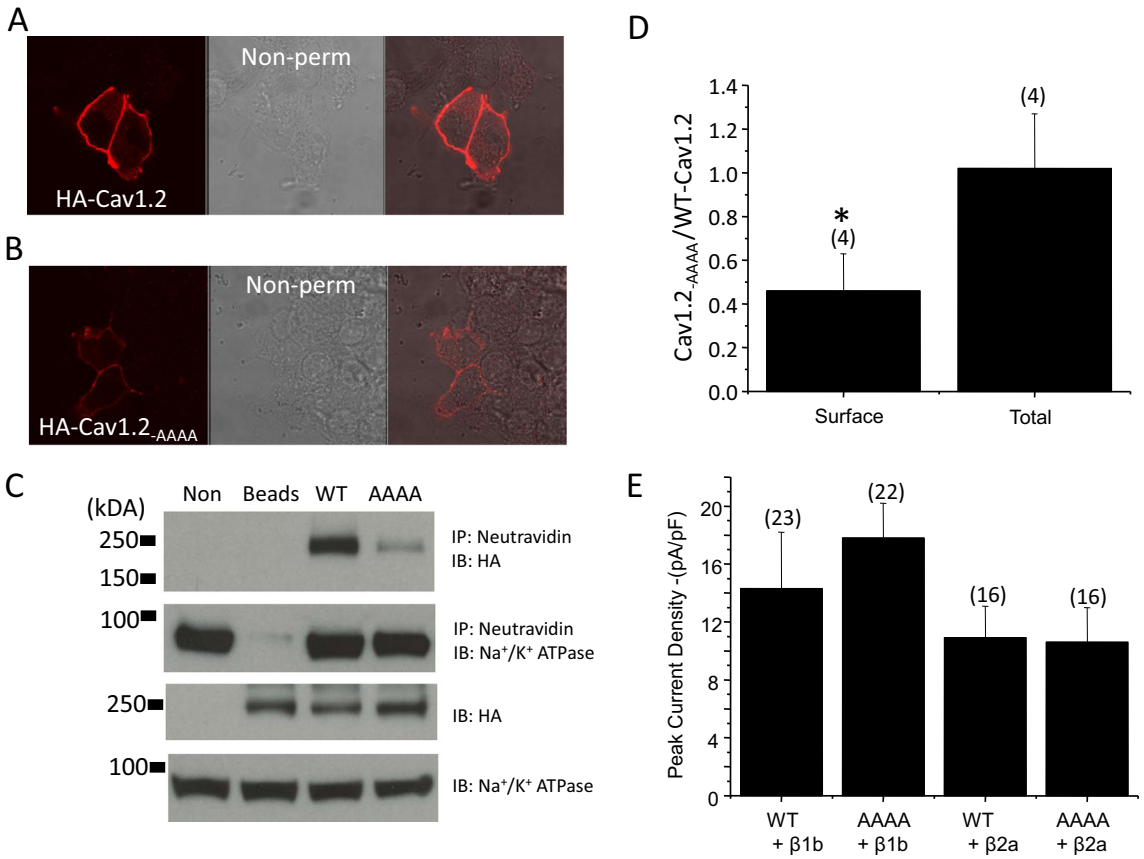

Fig. 5 Eliminating the CISI sequence from Cav1.2 channels reduces surface expression but not current density. **a** Non-permeabilzed tsA-201 cells expressing Cavβ1b/Cavα2δ with externally tagged HA-Cav1.2 (Alexa 594) or HA-Cav1.2-$_{AAAA}$ channels (**b**). **c** Biotinylation of HA tagged Cav1.2 (WT) and Cav1.2-$_{AAAA}$ channels (AAAA) expressed with Cavβ1b/α2δ in transfected tsA-201 cells and below, the same biotinylation stripped and reprobed for Na^+/K^+ ATPase. Controls are non-transfected and beads only. The third blot shows 100 μg of lysates probed for HA and below this, the same blot stripped and reprobed for Na^+/K^+ ATPase. **d** Quantification of biotinylated channels from **c** which shows that Cav1.2-$_{AAAA}$ channels express significantly less (0.46±0.17, *p=0.02 by Students t-test) at the cell surface compared to WT-Cav1.2, whereas it displays similar total protein expression. All data were first normalized to the levels of the ATPase control protein before ratios between the two channels were calculated. **e** A bar graph displaying peak current density of non-tagged Cav1.2 and Cav1.2-$_{AAAA}$ channels transiently expressed in tsA-201 cells with either Cavβ1b, or Cavβ2a and Cavα2δ. There is no significant difference in the current density of WT-Cav1.2 (−14.3±3.9 pA/pF) and Cav1.2-$_{AAAA}$ (−17.8±2.4 pA/pF) channels with Cavβ1b, or between WT-Cav1.2 (−10.9±2.2 pA/pF) and Cav1.2-$_{AAAA}$ (−10.6±2.4 pA/pF) with Cavβ2a

Cav1.2 channels lacking an N-terminal α-CaMKII binding site are more effectively facilitated by BayK 8644

The observation that whole-cell current densities of the quadruple alanine mutant were not different from those of wild type channels suggest that Cav1.2-$_{AAAA}$ channels either have an augmented single channel amplitude, or alternatively an increased open probability. The former possibility is highly unlikely given that the CaMK site is located far from the selectivity filter, leaving an increase in maximum open probability as a more likely scenario. To further explore the gating behavior of the mutant channels, we examined their facilitation by either voltage, or BayK 8644. As CaM kinase is linked to voltage-dependent facilitation (VDF) of L-type calcium channels [27], we first considered the possibility that Cav1.2-$_{AAAA}$ channels might be tonically facilitated. Figure 6a shows that Cavβ2a promotes a minimal 20 % increase in VDF of WT channels which is consistent with previous reports [7, 17]. Mutant channels showed voltage facilitation that was indistinguishable from that of WT with Cavβ2a. In contrast, Cavβ1b prevented facilitation of both channels in our hands, in contrast with previous studies [5, 32]. Altogether, the results in Fig. 6a indicate that Cav1.2-$_{AAAA}$ is not in a tonically facilitated state.

Next we tested whether Cav1.2-$_{AAAA}$ could be facilitated by application of BayK 8644 which is known to increase the open probability of L-type calcium channels [19, 33, 45]. Indeed, exogenous calcium insensitive CaMKII has also been shown to promote increased open probability of L-type calcium channels in ventricular myocytes, in analogy with the effects of BayK 8644 [42]. Figure 6b displays the current–voltage relationship for WT-Cav1.2 and Cav1.2-$_{AAAA}$ channels treated with 1 μM BayK 8644. Although both channels displayed increased whole cell current density upon treatment,

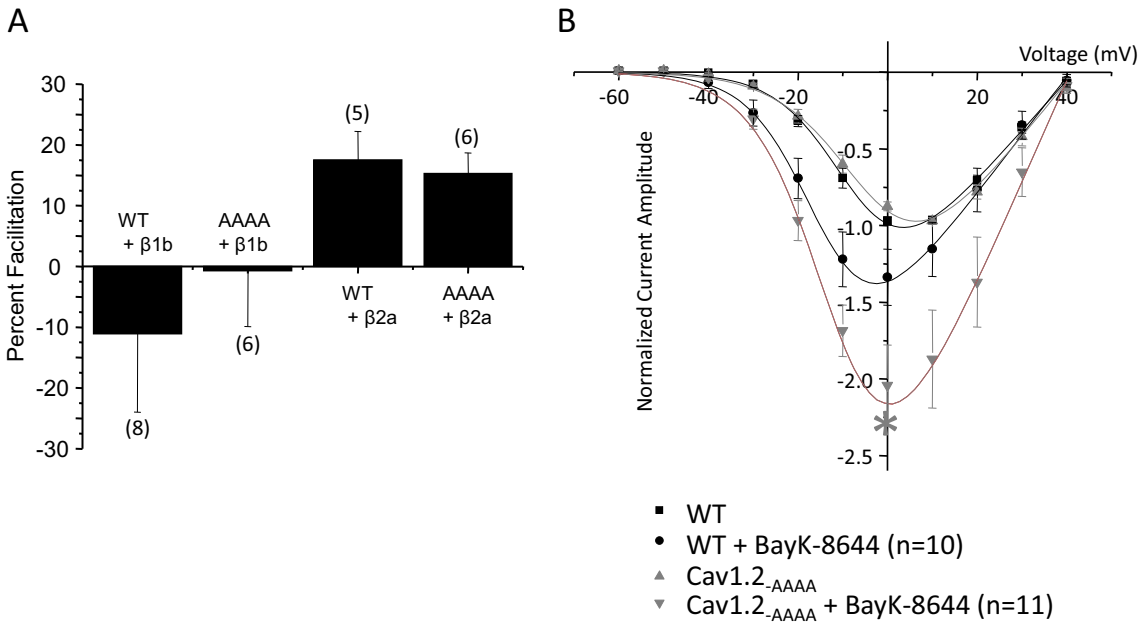

Fig. 6 Cav1.2$_{-AAAA}$ channels can be facilitated by BayK 8644 but not voltage. **a** A bar graph displaying percent change for voltage-dependent facilitation of non-tagged Cav1.2 and Cav1.2$_{-AAAA}$ channels transiently expressed in tsA-201 cells with Cavα2δ and either Cavβ1b or Cavβ2a. There is no significant difference in the percent facilitation by voltage for WT, or Cav1.2$_{-AAAA}$ channels with either Cavβ subunit. **b** Normalized current voltage relationships of non-tagged Cav1.2, or Cav1.2$_{-AAAA}$ channels expressed with Cavβ1b/Cavα2δ with and without 1 μM± BayK-8644. Cav1.2$_{-AAAA}$ channels show significantly more facilitation of peak current (asterisk) by±BayK-8644 (239±28 %, *$p \leq 0.04$ by Student's *t*-test) compared to WT-Cav1.2 channels (139±16 %). For both wild type and mutant channels, data were normalized to those obtained in the absence of BayK8644

Cav1.2$_{-AAAA}$ showed a much greater BayK 8644 -mediated increase (239±28 % at peak, *p=0.04 by Student's *t*-test) in current density compared to WT-Cav1.2 channels (139± 16 %). These data suggest that the inability of the mutant channel to bind CaMKII renders the channel more susceptible to the effects of BayK-8644, suggesting that CaMKII deficient channels can be opened more effectively.

Discussion

Cav1.2 and CaM kinase are important components of neuronal calcium signaling pathways. CaM kinase can associate with the C terminus of Cav1.2 and modulate CDF [22], but only when the IQ domain which anchors CaM is ablated [46]. We recently narrowed the position of an N-terminal CaMKII site in Cav1.2 [34] and in this work, have localized it to four residues (CISI) proximal to domain I of the channel. Full length channels lacking this CISI element (Cav1.2$_{-AAAA}$) display a significant reduction in surface expression, yet as well, an unexpected increase in function which offsets the trafficking defect. This motif does not appear to resemble CamKII interaction motifs found in other ion channels including the putative interaction site in the Cav1.2 C terminus. To our knowledge, there is no prior evidence in the literature for a role of CaM kinase in calcium channel trafficking, however it is worth noting that CaMKII does regulate trafficking of potassium channels to the cell membrane [29, 37, 38]. Also, removal of the Cav1.2 N terminus has been shown to increase surface expression of these channels in *Xenopus* oocytes indicating this region of the channel can participate in subcellular trafficking [39].

The observed compensatory increase in the functional properties of Cav1.2$_{-AAAA}$ could in principle be due to two mechanisms. On the one hand it is possible that Cav1.2$_{-AAAA}$ channels have a larger single channel conductance than WT-Cav1.2. However, given that the pool of Cav1.2$_{-AAAA}$ channels in the membrane is less than half of that of WT-Cav1.2 (Fig. 5d), this would imply that the single channel conductance of the Cav1.2$_{-AAAA}$ would need to double to account for the reduction in surface expression. This seems unlikely given that only the p-loops and outer vestibules of the pore (i.e., membrane spanning regions S5–S6 regions) have been shown to strongly impact selectivity [43] and permeation [9, 13, 44], whereas the N-terminal region, and more specifically, the CISI site, is far from these loci.

The possibility of an increase in maximum open probability of Cav1.2$_{-AAAA}$ is therefore the more likely scenario, and is supported by a number of considerations: First, we have previously measured the open probability of Cav1.2 channels at the single channel level and found it to be 0.07 at the peak of the current–voltage relation 0 mV [14], leaving considerable room for increase in the open probability of mutant channels.

Second, deletion of the first 46 amino acids in the N terminus of the cardiac Cav1.2 channel have been previously shown to affect maximum open probability without affecting the voltage dependence of gating (note that the voltage dependence of activation was not visibly affected by the alanine substitutions; see Fig. 6b) [24], suggesting the possibility that this stretch of residues might perhaps functionally interact with the newly identified CaMKII site. Finally, it is worth noting that a portion of the Cav1.2 C terminus which contains the C-terminal CaMKII site has been shown to regulate both channel trafficking and single channel open probability [25]. Although voltage-dependent facilitation was not different between the mutant and WT channels, BayK8644 appeared to more effectively augment the CaMKII binding deficient mutant channel. This implies that Cav1.2$_{-AAAA}$ may be susceptible to even greater increases in maximum open probability compared to wild type channels. We can only speculate as to how alterations in the channel's N terminus affect BayK8644 regulation of the channel. The amino acid residues involved in dihydropyridine binding are known to be localized to the domain III and IV S5 and S6 regions [36], which are located far from the N terminus in the linear sequence. However, other regions of the channel have been shown to affect dihydropyridine block of Cav1.2 channels, as evident from the distinct effects of nisoldipine on the smooth muscle and cardiac Cav1.2 isoforms [20]. Notably, these two channel isoforms exhibit differences in their N-terminal regions. How the N terminus region may be coupled to the actual dihydropyridine interaction sites is unclear but could potentially involve interactions between the N terminus and regions such as the C terminus that is associated with the domain IV S6 region. Alternatively, the N-terminal CaMKII site may simply be allosterically coupled to both the activation gating machinery and the BayK8644 interaction regions, thus accounting for the greater BayK8644 mediated facilitation of currents in the mutant channel.

At this point, it is unclear whether CaMKII modulation of native channels parallels our observations in tsA-201 cells, although it is tempting to speculate about the physiological significance of offsetting effects on channel trafficking and function to yield a similar net Cav1.2 whole cell current. One key function of neuronal Cav1.2 channels is the activation of calcium-dependent gene transcription events that are dependent on CaM interactions with the channel and downstream activation of CaMKII [42]. Importantly, this process is critically dependent on the open probability of individual channels [40]. A switch to fewer channels with increased open probability would therefore result in more effective excitation transcription coupling, without producing a net rise in calcium influx, and thus in increased risk of calcium toxicity [10]. In this regard CaMKII could act as a negative feedback regulator that reduces open probability upon association with the channel. This possibility will need to be explored experimentally in future studies.

Altogether, our data reveal a CaMKII site in the N terminus of Cav1.2 is formed by four proximal residues (CISI). In the full-length Cav1.2 channel, removal of CISI results in a decrease in surface expression, but an offsetting functional increase presumably due to an increase in maximum open probability. These data thus implicate a role for CaMKII in both channel trafficking and function.

Acknowledgments This work was supported by a grant from the Natural Sciences and Engineering Research Council. BAS is supported by a studentship from Alberta Innovates-Health Solutions (AI-HS). IAS is supported by a postdoctoral fellowship from Mitacs Elevate. GWZ is an AI-HS Scientist and a Canada Research Chair.

Conflict of interest The authors declare that they have no conflict of interest.

Ethical Standards All experiments performed in this manuscript comply with the laws of Canada.

References

1. Altier C, Dubel SJ, Barrere C, Jarvis SE, Stotz SC, Spaetgens RL, Scott JD, Cornet V, De Waard M, Zamponi GW, Nargeot J, Bourinet E (2002) Trafficking of L-type calcium channels mediated by the postsynaptic scaffolding protein AKAP79. J Biol Chem 277:33598–33603
2. Bading H, Ginty DD, Greenberg ME (1993) Regulation of gene expression in hippocampal neurons by distinct calcium signaling pathways. Science 260:181–186
3. Ben Johny M, Yang PS, Bazzazi H, Yue DT (2013) Dynamic switching of calmodulin interactions underlies Ca^{2+} regulation of CaV1.3 channels. Nat Commun 4:1717
4. Blaeser F, Sanders MJ, Truong N, Ko S, Wu LJ, Wozniak DF, Fanselow MS, Zhuo M, Chatila TA (2006) Long-term memory deficits in Pavlovian fear conditioning in Ca^{2+}/calmodulin kinase kinase alpha-deficient mice. Mol Cell Biol 26:9105–9115
5. Bourinet E, Charnet P, Tomlinson WJ, Stea A, Snutch TP, Nargeot J (1994) Voltage-dependent facilitation of a neuronal alpha 1C L-type calcium channel. EMBO J 13:5032–5039
6. Catterall WA (2011) Voltage-gated calcium channels. Cold Spring Harb Perspect Biol 3
7. Cens T, Mangoni ME, Richard S, Nargeot J, Charnet P (1996) Coexpression of the beta2 subunit does not induce voltage-dependent facilitation of the class C L-type Ca channel. Pflugers Arch 431:771–774
8. Christel C, Lee A (2012) Ca2+-dependent modulation of voltage-gated Ca^{2+} channels. Biochim Biophys Acta 1820:1243–1252
9. Cibulsky SM, Sather WA (2003) Control of ion conduction in L-type Ca^{2+} channels by the concerted action of S5–6 regions. Biophys J 84:1709–1719
10. Clapham DE (2007) Calcium signaling. Cell 131:1047–1058
11. de Maria CD, Soong TW, Alseikhan BA, Alvania RS, Yue DT (2001) Calmodulin bifurcates the local Ca^{2+} signal that modulates P/Q-type Ca^{2+} channels. Nature 411:484–489
12. Dick IE, Tadross MR, Liang H, Tay LH, Yang W, Yue DT (2008) A modular switch for spatial Ca^{2+} selectivity in the calmodulin regulation of CaV channels. Nature 451:830–834
13. Dirksen RT, Nakai J, Gonzalez A, Imoto K, Beam KG (1997) The S5–S6 linker of repeat I is a critical determinant of L-type Ca2+ channel conductance. Biophys J 73:1402–1409

14. Doering CJ, Hamid J, Simms B, McRory JE, Zamponi GW (2005) Cav1.4 encodes a calcium channel with low open probability and unitary conductance. Biophys J 89:3042–3048
15. Dolmetsch RE, Pajvani U, Fife K, Spotts JM, Greenberg ME (2001) Signaling to the nucleus by an L-type calcium channel–calmodulin complex through the MAP kinase pathway. Science 294:333–339
16. Graef IA, Mermelstein PG, Stankunas K, Neilson JR, Deisseroth K, Tsien RW, Crabtree GR (1999) L-type calcium channels and GSK-3 regulate the activity of NF-ATc4 in hippocampal neurons. Nature 401:703–708
17. Grueter CE, Abiria SA, Dzhura I, Wu Y, Ham AJ, Mohler PJ, Anderson ME, Colbran RJ (2006) L-type Ca^{2+} channel facilitation mediated by phosphorylation of the beta subunit by CaMKII. Mol Cell 23:641–650
18. Hamid J, Nelson D, Spaetgens R, Dubel SJ, Snutch TP, Zamponi GW (1999) Identification of an integration center for cross-talk between protein kinase C and G protein modulation of N-type calcium channels. J Biol Chem 274:6195–6202
19. Hofer GF, Hohenthanner K, Baumgartner W, Groschner K, Klugbauer N, Hofmann F, Romanin C (1997) Intracellular Ca^{2+} inactivates L-type Ca^{2+} channels with a Hill coefficient of approximately 1 and an inhibition constant of approximately 4 microM by reducing channel's open probability. Biophys J 73:1857–1865
20. Hu H, Marban E (1998) Isoform-specific inhibition of L-type calcium channels by dihydropyridines is independent of isoform-specific gating properties. Mol Pharmacol 53:902–907
21. Hudmon A, Lebel E, Roy H, Sik A, Schulman H, Waxham MN, De Koninck P (2005) A mechanism for Ca^{2+}/calmodulin-dependent protein kinase II clustering at synaptic and nonsynaptic sites based on self-association. J Neurosci 25:6971–6983
22. Hudmon A, Schulman H, Kim J, Maltez JM, Tsien RW, Pitt GS (2005) CaMKII tethers to L-type Ca^{2+} channels, establishing a local and dedicated integrator of Ca^{2+} signals for facilitation. J Cell Biol 171:537–547
23. Jeon D, Kim S, Chetana M, Jo D, Ruley HE, Lin SY, Rabah D, Kinet JP, Shin HS (2010) Observational fear learning involves affective pain system and Cav1.2 Ca^{2+} channels in ACC. Nat Neurosci 13:482–488
24. Kanevsky N, Dascal N (2006) Regulation of maximal open probability is a separable function of Ca(v)beta subunit in L-type Ca^{2+} channel, dependent on NH2 terminus of alpha1C (Ca(v)1.2alpha). J Gen Physiol 128:15–36
25. Kepplinger KJ, Kahr H, Forstner G, Sonnleitner M, Schindler H, Schmidt T, Groschner K, Soldatov NM, Romanin C (2000) A sequence in the carboxy-terminus of the alpha(1C) subunit important for targeting, conductance and open probability of L-type Ca(2+) channels. FEBS Lett 477:161–169
26. Langwieser N, Christel CJ, Kleppisch T, Hofmann F, Wotjak CT, Moosmang S (2012) Homeostatic switch in hebbian plasticity and fear learning after sustained loss of Cav1.2 calcium channels. J Neurosci 30:8367–8375
27. Lee TS, Karl R, Moosmang S, Lenhardt P, Klugbauer N, Hofmann F, Kleppisch T, Welling A (2006) Calmodulin kinase II is involved in voltage-dependent facilitation of the L-type Cav1.2 calcium channel: identification of the phosphorylation sites. J Biol Chem 281:25560–25567
28. Lee A, Zhou H, Scheuer T, Catterall WA (2003) Molecular determinants of Ca(2+)/calmodulin-dependent regulation of Ca(v)2.1 channels. Proc Natl Acad Sci U S A 100:16059–16064
29. Li J, Marionneau C, Koval O, Zingman L, Mohler PJ, Nerbonne JM, Anderson ME (2007) Calmodulin kinase II inhibition enhances ischemic preconditioning by augmenting ATP-sensitive K^+ current. Channels (Austin) 1:387–394
30. Mizuno K, Ris L, Sanchez-Capelo A, Godaux E, Giese KP (2006) Ca^{2+}/calmodulin kinase kinase alpha is dispensable for brain development but is required for distinct memories in male, though not in female, mice. Mol Cell Biol 26:9094–9104
31. Perez-Reyes E, Castellano A, Kim HS, Bertrand P, Baggstrom E, Lacerda AE, Wei XY, Birnbaumer L (1992) Cloning and expression of a cardiac/brain beta subunit of the L-type calcium channel. J Biol Chem 267:1792–1797
32. Platano D, Qin N, Noceti F, Birnbaumer L, Stefani E, Olcese R (2000) Expression of the alpha(2)delta subunit interferes with prepulse facilitation in cardiac L-type calcium channels. Biophys J 78:2959–2972
33. Schmid R, Seydl K, Baumgartner W, Groschner K, Romanin C (1995) Trypsin increases availability and open probability of cardiac L-type Ca^{2+} channels without affecting inactivation induced by Ca^{2+}. Biophys J 69:1847–1857
34. Simms BA, Souza IA, Zamponi GW (2013) A novel calmodulin site in the Cav1.2 N-terminus regulates calcium-dependent inactivation. Pflugers Arch. doi:10.1007/s00424-013-1423-9
35. Simms BA, Zamponi GW (2014) Neuronal voltage-gated calcium channels: structure, function, and dysfunction. Neuron 82:24–45
36. Sinnegger MJ, Wang Z, Grabner M, Hering S, Striessnig J, Glossmann H, Mitterdorfer J (1997) Nine L-type amino acid residues confer full 1,4-dihydropyridine sensitivity to the neuronal calcium channel alpha1A subunit. Role of L-type Met1188. J Biol Chem 272:27686–27693
37. Varga AW, Yuan LL, Anderson AE, Schrader LA, Wu GY, Gatchel JR, Johnston D, Sweatt JD (2004) Calcium-calmodulin-dependent kinase II modulates Kv4.2 channel expression and upregulates neuronal A-type potassium currents. J Neurosci 24:3643–3654
38. Wagner S, Hacker E, Grandi E, Weber SL, Dybkova N, Sossalla S, Sowa T, Fabritz L, Kirchhof P, Bers DM, Maier LS (2009) Ca/calmodulin kinase II differentially modulates potassium currents. Circ Arrhythm Electrophysiol 2:285–294
39. Wei X, Neely A, Olcese R, Lang W, Stefani E, Birnbaumer L (1996) Increase in Ca^{2+} channel expression by deletions at the amino terminus of the cardiac alpha 1C subunit. Receptors Channels 4:205-15
40. Wheeler DG, Barrett CF, Groth RD, Safa P, Tsien RW (2008) CaMKII locally encodes L-type channel activity to signal to nuclear CREB in excitation–transcription coupling. J Cell Biol 183:849–863
41. Wu GY, Deisseroth K, Tsien RW (2001) Activity-dependent CREB phosphorylation: convergence of a fast, sensitive calmodulin kinase pathway and a slow, less sensitive mitogen-activated protein kinase pathway. Proc Natl Acad Sci U S A 98:2808–2813
42. Wu Y, Dzhura I, Colbran RJ, Anderson ME (2001) Calmodulin kinase and a calmodulin-binding 'IQ' domain facilitate L-type Ca^{2+} current in rabbit ventricular myocytes by a common mechanism. J Physiol 535:679–687
43. Yang J, Ellinor PT, Sather WA, Zhang JF, Tsien RW (1993) Molecular determinants of Ca^{2+} selectivity and ion permeation in L-type Ca^{2+} channels. Nature 366:158–161
44. Yatani A, Bahinski A, Wakamori M, Tang S, Mori Y, Kobayashi T, Schwartz A (1994) Alteration of channel characteristics by exchange of pore-forming regions between two structurally related Ca^{2+} channels. Mol Cell Biochem 140:93–102
45. Yoshino M, Someya T, Nishio A, Yazawa K, Usuki T, Yabu H (1989) Multiple types of voltage-dependent Ca channels in mammalian intestinal smooth muscle cells. Pflugers Arch 414:401–409
46. Zuhlke RD, Pitt GS, Deisseroth K, Tsien RW, Reuter H (1999) Calmodulin supports both inactivation and facilitation of L-type calcium channels. Nature 399:159–162